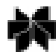
Optical and Quantum Electronics **32:** 553–571, 2000.
© 2000 *Kluwer Academic Publishers. Printed in the Netherlands.*

Ultrafast response of multi-energy proton-bombarded GaAs photoconductors

G.-R. LIN[1] AND C.-L. PAN[2]
[1]*Institute of Electro-Optical Engineering, Tatung University, 40 Chung Shan North Rd, Sect. 3, Taipei 10451, Taiwan, ROC (E-mail: grlin@ttu.edu.tw);*
[2]*Institute of Electro-Optic Engineering, National Chiao Tung University, 1001 Ta Hsueh Rd., Hsinchu 30010, Taiwan, ROC (E-mail: clpan@cc.nctu.edu.tw)*

Abstract. We have investigated the ultrafast optical and optoelectronic characteristics of multi-energy proton-bombarded GaAs (GaAs:H^+) material and devices in some detail. Photo-excited carrier lifetimes of GaAs:H^+ were observed to be as low as 350 ± 50 fs. Photoconductive switches (PCS) fabricated on GaAs:H^+ were found to exhibit lower dark currents (15 nA at a bias of 10 V) and higher breakdown voltage (> 100 kV/cm) than PCS's fabricated on semi-insulating (S.I.) GaAs. The temporal response of the GaAs:H^+ PCS was about 2 ps at full-wave half minimum. Optically excited terahertz (THz) radiation from GaAs:H^+ was reported for the first time to our knowledge. The temporal response and spectral bandwidth of the emitted THz radiation were 0.7 ps and 1.25 THz, respectively. The field strength of the THz signal was about 20 mV/cm. From the THz data, we are able to deduce that the effective carrier mobility of GaAs:H^+ was less than 1 cm^2/V-sec.

Key words: carrier lifetime, electro-optic sampling, photoconductor, proton-bombarded GaAs, THz radiation

1. Introduction

Photoconductors with ultrashort photo-excited carrier lifetime, good optical responsivity, high breakdown field and low dark current are essential for ultrafast optoelectronic switching applications (Chen *et al.* 1991; Warren *et al.* 1991; Chou *et al.* 1992; Verghese *et al.* 1996). Various classes of semiconductors, e.g., intrinsic, impurity-dominated, radiation-damaged, polycrystalline and amorphous, have been explored as ultrafast photoconductors (Anon. 1993). In the past decades, non-stoichiometric GaAs and related compound semiconductors (Anon. 1990, 1993) have been the material of choice for the applications mentioned above. GaAs film grown at a relatively low substrate temperatures by molecular beam epitaxy (MBE) (Smith *et al.* 1989), usually referred to as LT-GaAs, is an excellent example of this type of material (Look *et al.* 1990; Lochtefeld 1996). Recently, an alternative material (GaAs:As^+), which is also an arsenic-rich GaAs material the same as LT-GaAs, prepared by implanting dense arsenic ions was pursued successfully by several groups (Claverie *et al.* 1993a, b; Ganikhanov *et al.* 1995). Ion implantation is a mature technology more widely available than MBE.

It is also compatible with GaAs integrated circuit (IC) technology. Because arsenic ion is heavy, the implanting energy as large as 1 MeV is required for the arsenic ions to penetrate and generate trapping centers deep into the GaAs substrate (Krotkus *et al.* 1995). High-energy implantation is beneficial for sharpening the tail response of photoconductive switches (PCS's) fabricated on GaAs:As$^+$. This is, however, achieved at a cost of serious degradation of sample crystallinity (Kaminska *et al.* 1989; Claverie *et al.* 1993a), carrier mobility (Look *et al.* 1990; Krotkus *et al.* 1995), and resistivity (Look *et al.* 1990; Lin *et al.* 1994). As a result, as-grown (or as-implanted) arsenic-rich GaAs materials are unsuitable for fabrication of low-leakage and high-gain photoconductive switches (Wang *et al.* 1996; Lin and Pan 1997; Lin *et al.* 1998). Appropriate thermal annealing process is often required, with the temporal response degraded to somewhat. Nonetheless, one alternative would be to employ lighter ions such as the proton. In fact, proton-bombarded GaAs (or GaAs:H$^+$) material has been studied extensively in the past (Chou *et al.* 1992; Warren *et al.* 1991; Verghese *et al.* 1996; Anon. 1993). The rise time (10 to 90% of the peak amplitude) and temporal response (Full width at half maximum, FWHM) of single-dose GaAs:H$^+$ PCS were reported to be 3.2 and 4.5 ps, respectively. It was also suggested by Johnson *et al.* (1989) that a recipe of implantation with higher dose of protons and a smaller size of photoconductive gap could further reduce the carrier lifetime and switching response of GaAs:H$^+$ PCS. Subsequently, Lambsdorff *et al.* (1991) reported the decreasing trend of carrier lifetime as the implantation dosage increased. With an optical injection energy of 2.3 eV, the lifetime of photo-excited carriers in multi-dose GaAs:H$^+$ sample was found to reach a lower limit at about 0.5 ps beyond an amorphization dosage of 1.4×10^{15} ions/cm^2 (Lambsdroff *et al.* 1991). Significantly, it was found from the current–voltage characteristics of Au-GaAs:H$^+$ contacts that the GaAs substrate can be fully passivated (electrically isolated) via an appropriate selection of the proton implantation recipe (Ejimanya 1986). This indicates that as-implanted GaAs:H$^+$ can also be highly resistive. Furthermore, both a deeper and a more uniform distribution of damage-induced trapping centers are mandatory due to the relatively large absorption depth (the $1/e$ penetration length of the photon) of the GaAs material. These findings indicate that improvements on both electrical and ultrafast optoelectronic properties of the GaAs:H$^+$ photoconductive devices, such that they are competitive with arsenic-rich GaAs photoconductors.

In this paper, GaAs:H$^+$ material prepared by using a single-dose multi-energy recipe to achieve deep and uniform implantation is proposed and demonstrated for ultrafast optoelectronic applications. An extensive array of diagnostic tools such as current–voltage measurement, time-resolved reflectivity, external electro-optic sampling and optically-excited THz radiation

were utilized. In particular, the last item was reported for the first time to our knowledge. It allows us to determine the carrier mobility of this heavily-damaged material. The radiation mechanism of optically-excited THz radiation from GaAs:H^+ was also elucidated.

2. Experimental

The GaAs:H^+ samples were prepared by implanting the liquid-encapsulated-Czochralski (LEC) grown, (1 0 0)-oriented semi-insulating (S.I.) GaAs substrates ($\rho > 10^7$ Ω-cm) with 50, 100 and 200 keV proton at the dosage of 10^{16} ions/cm^2 in a commercial apparatus (Varian E220). Typical current density value was 1 mA/cm^2 and the exposure time was 10–15 min. This process was repeated several times to attain the desired dosage. The implantation depth is estimated to be up to 2 μm from TRIM simulations. PCS's with a gap of 20 μm were fabricated and integrated with 2-cm long coplanar waveguide (CPW) or coplanar stripline (CPS) transmission lines. The characteristic impedances of CPW and CPS structures are 50 and 75 Ω, respectively. Au/Ti (0.5/0.3 μm) metals were evaporated as the Schottky contacts of the PCS. A rapid-thermal alloying process at 300°C for 60 s was used to improve the adhesion of the contacts. The current voltage (I–V) characteristics of GaAs:H^+ PCS were measured by using an HP4145B semiconductor parametric analyzer.

The ultrafast photo-excited carrier lifetimes of GaAs:H^+ were determined by femtosecond time-resolved reflectivity measurements. The experimental setup is the same as described in our previous works (Ganikhanov *et al.* 1995; Lin and Pan 1997; Lin *et al.* 1998). The light source was a home-made, passively mode-locked Ti:sapphire/HITCI + IRI40 laser, which generates 100-fs wide optical pulse train at a repetition frequency of 82 MHz. The polarizations of pump and probe beams were perpendicular and the power ratio was 50/1 (400/8 mW). The laser wavelength was tuned to 865 nm. The photon energy is only about 9 meV higher than the bandgap of GaAs (≅1.424 eV). This was chosen to prevent either the intervalley scattering process of the photo-excited carriers from Γ band to the satellite band (usually the L band, $\Delta E_{\Gamma-L} = 300$ MeV) in momentum space, or the longitudinal optical phonon emission process ($\Delta E_{LO} = 36$ meV). Thus the influences of intraband relaxation and phonon scattering processes can also be ignored in our experiments. The energy of the pump pulses mechanically chopped at 3.2 kHz was about 4 ± 0.5 nJ. This corresponds to an injection density of photo-excited carriers of about 1×10^{19} cm^{-3}. The time resolution and detection sensitivity of our pump-probe apparatus were ≈150 fs and better than one parts in 10^5, respectively. The sensitivity of the time-resolved reflectivity measurement is the minimum detectable change in $\Delta R/R$ of samples, which depends on both

the intensities of pump and probe beams. However, the minimum signal can only be detected at pump intensity of larger than 20 mW. The fractional change of the reflected probe beam is detected by using a pair of large area Si p-i-n diodes operated in differential-detection mode and subsequently processed in a lock-in amplifier operated in a (R, θ) mode. An un-modulated laser beam was split from the probe beam and incident into one of the balanced (differential) photodetectors. The power of the un-modulated laser beam was tuned to offset the output DC level of the balanced (differential) photodetectors. This setup helps suppress the laser noise at the modulation frequency, therefore the signal-to-noise of the current apparatus can be further improved.

The ultrafast switching responses of the PCS's were examined by using an external electro-optic sampling (EEOS) system, as shown in Fig. 2 (Lin and Pan 1997; Lin *et al.* 1998). The femtosecond Ti:sapphire laser source was operated at 800 nm for this experiment. The pump power incident on the PCS was 140 mW while the probe power was 5 mW or less. The reflective-mode electro-optic sampling module consists of a polarization beam splitter (PBS), a quarter-wave plate (QWP), a half-wave plate (HWP), and a homemade $LiTaO_3$ electro-optic probing crystal located upon the GaAs:H^+ PCS. The thickness of the $LiTaO_3$ probe was polished down to 60 μm. A pair of Si p-i-n photodiodes differentially detected the phase change of the probe beam due to the optically generated electrical pulse. An equivalent-time sampling technique was utilized to determine the switching response of the

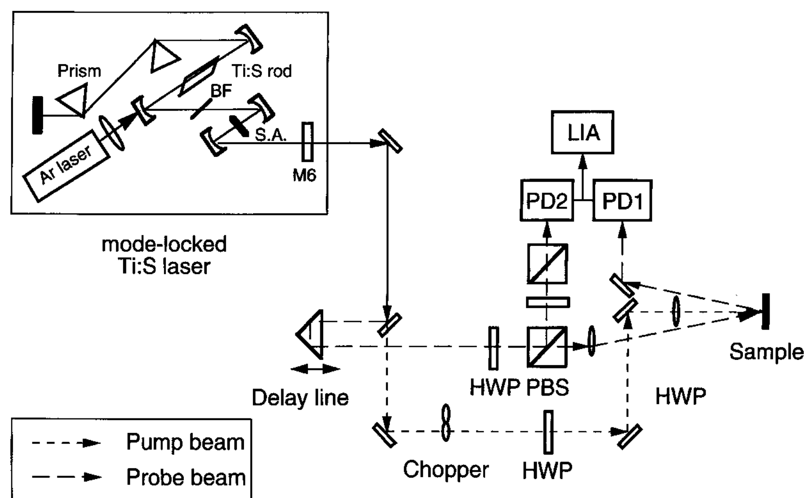

Fig. 1. Schematic diagram of a standard pump-probe system for measuring the time-solved optical reflectivity. BF: bandpass filter; S.A.: saturable absorber; PBS: polarized beam splitter; HWP: half-wave plate; QWP: quarter-wave plate; PD1 and PD2: photodetectors; LIA: lock-in amplifier.

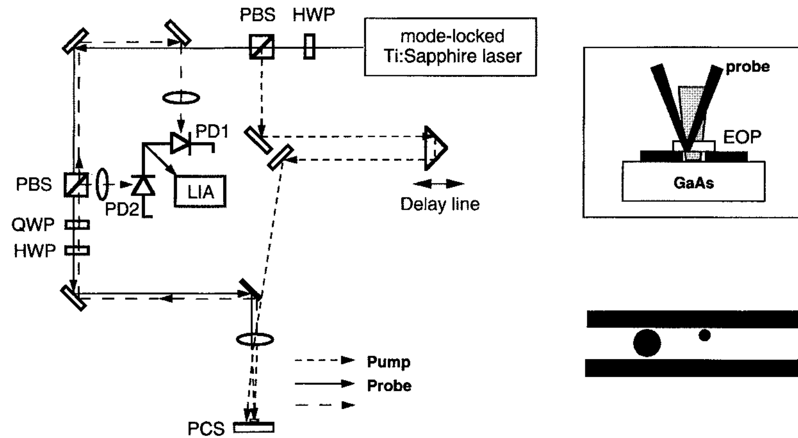

Fig. 2. The setup of an external electro-optic sampling (EEOS) system for measuring the switching response of ultrafast optoelectronic devices. PBS: polarized beam splitter; HWP: half-wave plate; QWP: quarter-wave plate; PD1 and PD2: photodetectors; LIA: lock-in amplifier; PCS: photoconductive switch; EOP: electro-optic probe crystal.

PCS. The temporal and spatial resolutions of current system are approximately about 0.9 ps and 5 μm, respectively.

For time-resolved detection of optically excited THz radiation (OETR) from GaAs:H^+, we employed the electro-optic field sensing technique (Wu and Zhang 1996). The experimental setup is shown in Fig. 3. A 1.5-mm thick, (1 1 0)-oriented ZnTe crystal was used as the THz field sensor. The power ratio between pump to probe was about 1000 or larger. A 90%-transparent pellicle beamsplitter was employed to collimate the focused probe beam

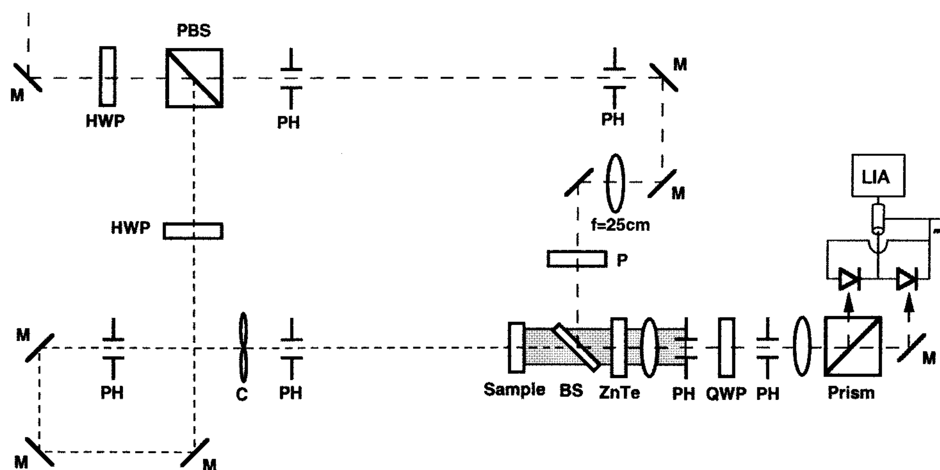

Fig. 3. The external electro-optic sensing system for detection the electric field of the freely propagated, optically excited THz radiation from GaAs:H^+ surface. M: mirror; PH: pin hole; P: polarizer; BS: beam splitter; HWP: half-wave plate; QWP: quarter-wave plate; LIA: lock-in amplifier.

along the propagation direction of the THz beam. The maximum and minimum THz radiation was obtained with the surface normal of sample tilting from the optical axis at tilting angles θ_t of about 70° and 0°, respectively (Zhang *et al.* 1990). A magnetic field of 0.32 Tesla was applied to measure the OETR signal at $\theta_t = 0°$.

3. Ultrafast optical studies of GaAs:H$^+$

The normalized transient reflectively change ($\Delta R/R$) of the GaAs:H$^+$ sample implanted with the single dosage and multi-energy recipe is shown in Fig. 4. A rigorous deconvoulution process that takes into account the residual effects of coherent interaction between the pump and probe beams (denoted as $\alpha(t)$) and the response of the GaAs:H$^+$ sample (denoted as $\beta(t)$) to optical excitation by a laser pulse of finite width was adopted. The normalized transient reflectivity change ($\Delta R/R$) can then be written as

$$\begin{aligned}\frac{\Delta R(t)}{R} &= C_1 \cdot \alpha(t) + C_2 \cdot \beta(t)\\ &= C_1 \int_{-\infty}^{\infty} I(t+t'') \cdot I(t'')\mathrm{d}t''\\ &\quad + C_2\left[\int_{-\infty}^{\infty} I(t+t') \cdot \left(\int_{-\infty}^{\infty} \gamma(t'+t'') \cdot I(t'')\mathrm{d}t''\right)\mathrm{d}t'\right] \end{aligned} \quad (1)$$

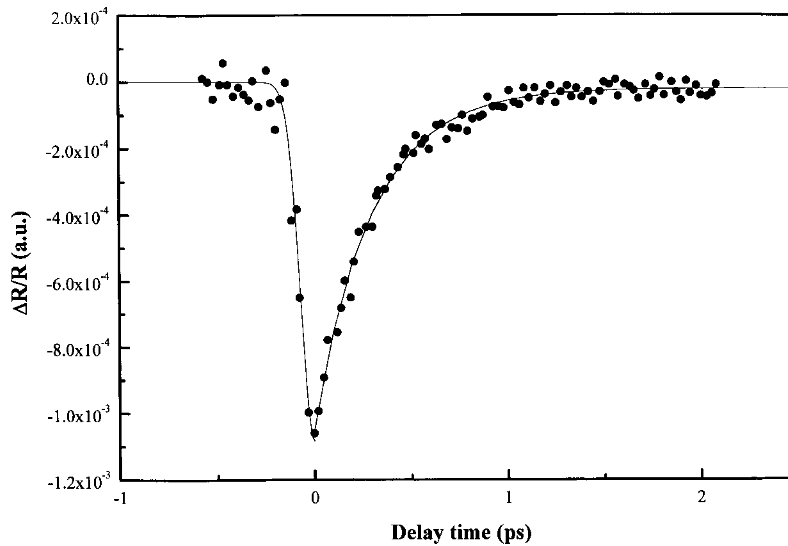

Fig. 4. The transient reflectivity change ($\Delta R/R$) data of the GaAs:H$^+$ implanted at single dosage and multi-energy recipe (solid circle) and the fitting curve (solid line).

$$\gamma(t'+t'') = \begin{cases} 0, & t'+t'' < 0 \\ \sum_{n=1}^{k} \gamma_n e^{-(t'+t'')/\tau_n}, & t'+t'' \geq 0 \end{cases}$$

where $I(t)$ is the intensity of the laser pulse; $\gamma(t)$ is the impulse response of the material in the form of a single or multiple exponential decay function; τ_n's are the lifetime of scattering, trapping, relaxation, and recombination processes of the photo-excited carriers in GaAs:H^+. In general, the pump and probe beams are orthogonally polarized. Further, the temporal duration of the laser pulse is far smaller than the semiconductor response and can be treated like a delta function. Equation (1) then reduces to

$$\frac{\Delta R(t)}{R(t)} \approx C_0 \sum_{n=1}^{k} \gamma_n e^{-t/\tau_n} \tag{2}$$

Analyzing Fig. 4 using the above procedures, we deduce that the carrier lifetime, τ_c of GaAs:H^+ is about 350 $\pm$ 50 fs. Both of the two equation, Equations (1) and (2) have been employed for analyzing the time-resolved reflectivity of GaAs:H^+ sample. In our case, the lifetime is three times larger than the pulsewidth of the laser. We found that the deviation between the fitted carrier lifetimes by using Equations (1) and (2) can be less than $\pm$10 fs in this condition. This is even smaller than the estimation error caused by fluctuations of time-resolved $\Delta R/R$ traces during measurements. Our result is consistent with these earlier experiments on GaAs:H^+ and comparable to τ_c's reported for a number of ultrafast photoconductors (Lambsdroff *et al.* 1991). These are summarized in Table 1. For example, the carrier lifetimes of GaAs samples implanted with 200 keV arsenic ions at dosages of 10^{12} to 10^{16} ions/cm^2 are about 0.19–0.26 ps (Ganikhanov *et al.* 1995). McIntosh *et al.* (1997) have also reported that the relaxation time of photo-excited carriers in as-grown LT-GaAs material epitaxial at 210°C was evaluated to be shorter than 200 fs by using TRPR measurement. Previously, we have shown that the ultrashort carrier lifetime in LT-GaAs (Lochtefeld 1996) or GaAs:As^+ (Lin *et al.* 1998) is caused by the large amount of unprecipated arsenic ions with associated $[As^0_{Ga}]$ antisite defects with activation energy $E_a \cong 0.64$ eV at densities of up to 10^{20} cm^{-3} in the samples (Lin *et al.* 1994). In analogy to correlation of defect concentration with ultrafast carrier lifetimes in GaAs:As^+ and LT-GaAs (Lochtefeld 1996), it is plausible that the ultrafast carrier dynamics in GaAs:H^+ material is also contributed by the presence of ultrahigh density of deep-level defect states. That is, the EL2-like defects with a slightly different activation energy of E_a = 0.82 eV (Ejimanya 1986). Following the Shockley–Read–Hall theory (Smith 1978; Esser *et al.* 1990), $\tau_c = [N_d \sigma V_{th}]^{-1}$, where N_d is the concentration of the trapping centers, σ is the

captured cross-section of photo-excited carriers, and V_{th} is the thermal velocity of GaAs material. For the EL2-like defects in GaAs:H^+, $\sigma \approx 1.1 \times 10^{-13}$ cm^{-2} (Tan *et al.* 1995). If we assume V_{th} of ion-implanted GaAs materials is about the same order of magnitude, we can estimate that the density of trapping centers in GaAs:H^+ is $\approx$3–5 $\times 10^{19}$ cm^{-3}, which is about half as large as that of arsenic antisite As^0_{Ga} defects in as-implanted GaAs:As^+ material. The slightly lower density of trapping centers in GaAs:H^+ than that in GaAs:As^+ can therefore adequately explain the relative magnitudes of the carrier lifetimes of the two materials. These results also suggest that 5×10^{18} cm^{-3} is the lowest concentration of trapping centers required for reduction of carrier lifetime of GaAs material to less than 1 ps (Lin *et al.* 1998).

From Fig. 4, we also determine that the maximum change in transient optical reflectivity ($\Delta R/R$) is -1×10^{-3}. The corresponding transient refractive index change, $\Delta n \approx -3 \times 10^{-3}$, is evaluated by using the simplified Kramers–Kronig relation (Esser *et al.* 1990). That is,

$$\begin{aligned}\frac{\Delta R}{R} &= \frac{4(n^2 - k^2 - 1)}{(n^2-1)^2 + k^2(1+n^2+k^2)}\Delta n + \frac{8nk}{(n^2-1)^2 + k^2(1+n^2+k^2)}\Delta k \\ &\approx \frac{4}{(n^2-1)}\Delta n + \frac{8nk}{(n^2-1)^2}\Delta k \\ &\cong \frac{4}{(n^2-1)}\Delta n \end{aligned} \tag{3}$$

where

$$R = \left[\frac{1-(n+ik)}{1+(n+ik)}\right]^2 = \frac{(1-n)^2 + k^2}{(1+n)^2 + k^2} \tag{4}$$

n and k are the real and imaginary part of the complex refractive index of GaAs:H^+. In comparison, the $\Delta R/R$ and Δn for GaAs:H^+ is comparable to those of GaAs:As^+ at annealing temperatures lower than 600°C (Lin *et al.* 1998), while significantly larger than those for as-implanted GaAs:As^+ (-5×10^{-4} and -2×10^{-3}, respectively) (Ganikhanov *et al.* 1995).

4. Optoelectronic characterization of GaAs:H^+ photoconductive switches

In Fig. 5, we have plotted the electro-optically sampled electrical waveform generated by the CPW-type proton-bombarded GaAs PCS. The rise time was

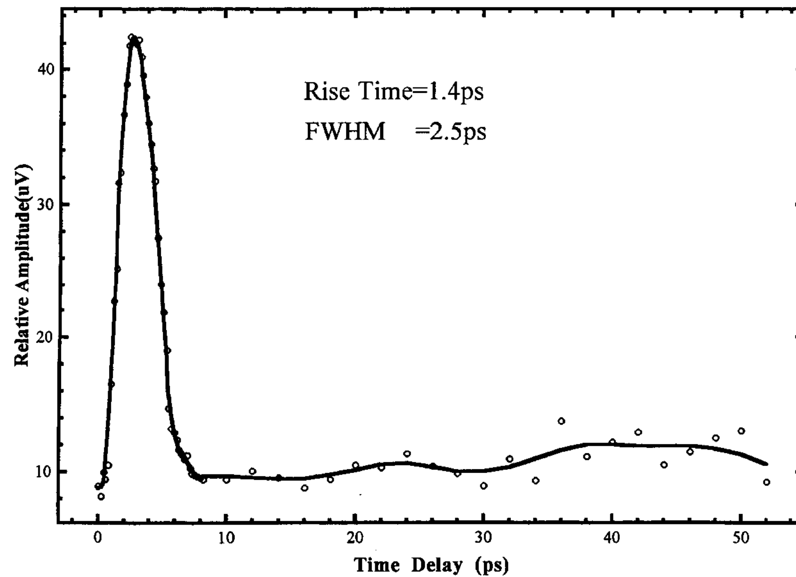

Fig. 5. The electro-optic sampled waveform of the optically generated electrical pulse from CPW-typed $GaAs{:}H^+$ PCS (○).

1.4 ps while the FWHM (full-width-half-maximum) was 2.5 ps. The risetime is slightly larger than our estimation of system resolution (0.9 ps). We attribute this partly to the fact that the probe point was about 6 mm away from the photoconductive gap. This results in dispersion and distortion of the high frequency components of the electrical pulse propagating on the CPW. With the sliding contact geometry of a CPS-type $GaAs{:}H^+$ PCS and probe at 1 mm from the photoconductive gap, we are able to reduce the FWHM of the switching response to 2 ps with a risetime of 1.2 ps (see Fig. 6). The corresponding 3 dB bandwidth of the CPS $GaAs{:}H^+$ PCS is greater than 150 GHz. This was obtained by fast-Fourier-transforming, the switching response of the CPS-type $GaAs{:}H^+$ PCS, as shown in Fig. 7. Previously, Schumacher *et al.* (1987) have shown that the PCS made on multi-dose and multi-energy implanted $GaAs{:}H^+$ substrate exhibit switching response of about 7.2 ps. Possibly, the long photoconductive tail response is due to the relatively low-dose recipe ($\approx 10^{12}$ ions/cm^2) they used. In comparison, Wang *et al.* (1996) has reported that the response time of the same device fabricated on $GaAs{:}As^+$ substrate annealed at 600°C for 15 s was measured to be of 1.23 ps (FWHM). Not long ago, we also demonstrated that the risetime and switching response of the furnace-annealed CPS-typed $GaAs{:}As^+$ PCS were evaluated to be about 2.2 and 3 ps, respectively (Lin and Pan 1997; Lin *et al.* 1998). Thus the temporal response of $GaAs{:}H^+$-based PCS is competitive to the PCS's made on arsenic-rich GaAs substrates.

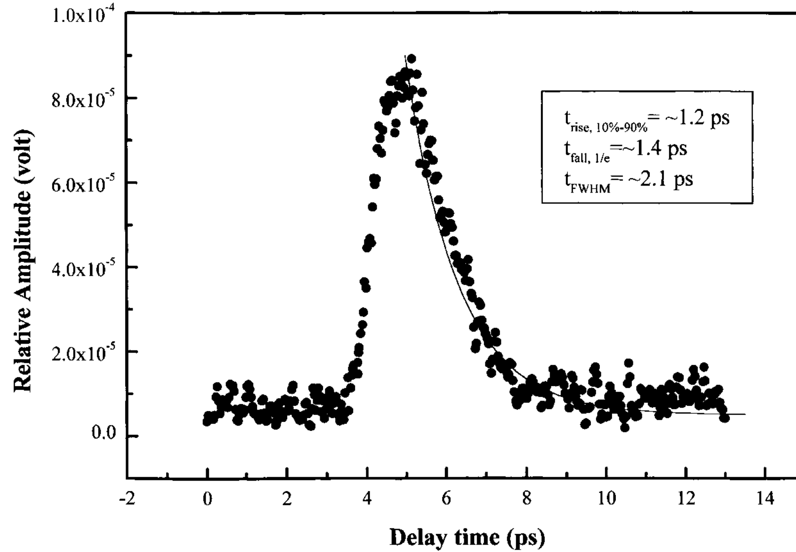

Fig. 6. The electro-optic sampled waveform of the optically generated electrical pulse from CPS-typed GaAs:H$^+$ PCS (●).

The dark current characteristic of an as-implanted, CPW-type GaAs:H$^+$ PCS is shown in Fig. 8. At a biased voltage of $V_{\text{bias}} = 10$ V (or $E_{\text{bias}} =$ 20 kV/cm), we find that the dark current was as low as 15 nA. The leakage current gradually increases with the biased voltage, up to 50 nA at $V_{\text{bias}} =$ 40 V. Such low dark current with no distinguished turn-on feature in the high bias region implies that the as-implanted GaAs:H$^+$ PCS's can sustain much

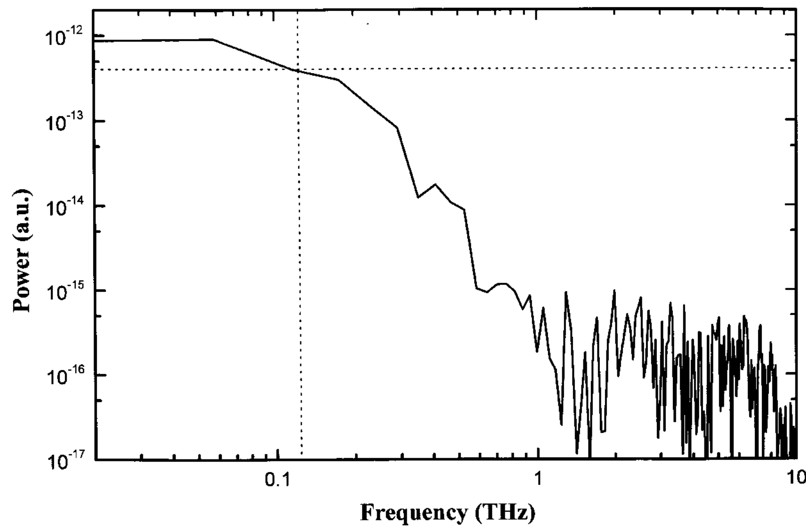

Fig. 7. The 3 dB bandwidth of the CPS GaAs:H$^+$ PCS converted from Fig. 6 by Fast Fourier Transform.

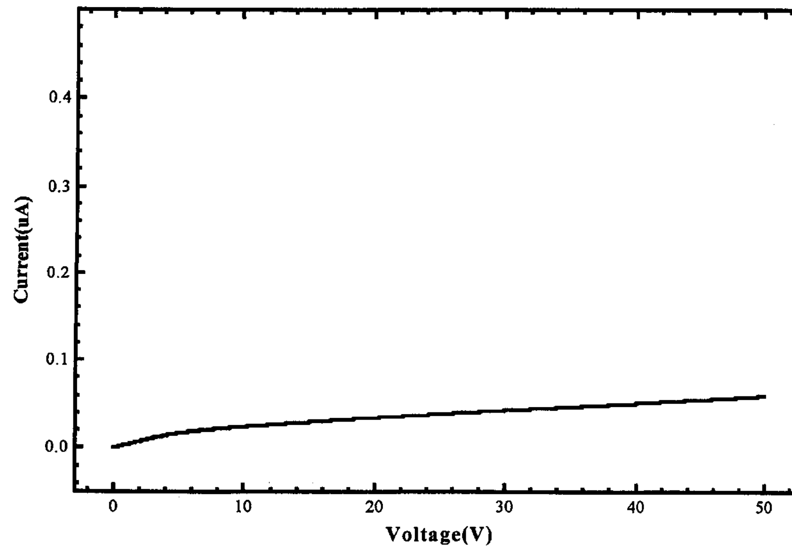

Fig. 8. The leakage I–V characteristic of an as-implanted, CPW-typed GaAs:H^+ PCS.

higher electric field before the device breaks down. In comparison, similar high resistivity is achieved in GaAs:As^+ only after long term post-implantation thermal annealing (>30 min) (Lin *et al.* 1998). The dark current of a CPW-type PCS fabricated on semi-insulating (S.I.) GaAs is shown in Fig. 9. We find I_{dc} for S.I. GaAs increased sharply with the biased voltage, up to 1 mA at $V_{bias} = 9$ V. Further, we note that the dark current of the GaAs:H^+ PCs is slightly larger than that of a S.I. GaAs PCS for $V_{bias} \leq 4$ V. The origin of this phenomenon is still under investigation. It is highly like that this is related to the highly concentrated deep-level defects in GaAs:H^+.

The photocurrents of GaAs:H^+ PCS at different optical injection levels are plotted as a function of bias voltage in Fig. 10. The responsivity of the GaAs:H^+ PCS biased at 10 V and illuminated with an average power of 25 mW was 1.2 mA/W. This is comparable to the performance of the devices made on other defect-rich materials such as LT-GaAs, GaAs:As^+, etc. (Lin *et al.* 1998). Such low responsivity can be attributed to the extremely low carrier mobility of the GaAs:H^+ material, estimated to be less than 1 cm^2/V-sec (see Sect. 5).

5. Optically excited THz radiation from GaAs:H^+

Terahertz radiation generated by femtosecond optical excitation of semiconductors and other materials has been an active field of ultrafast optoelectronics recently (Zhang *et al.* 1990; Wu and Zhang 1996). This technique

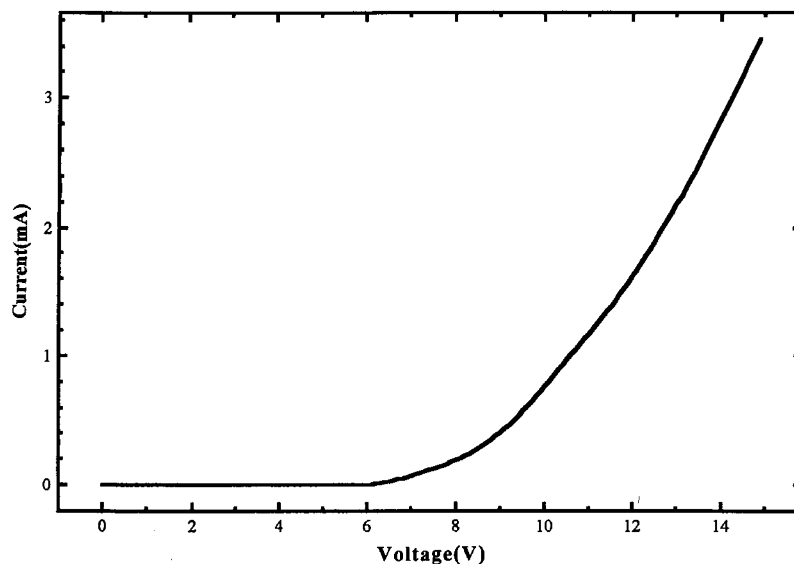

Fig. 9. The dark current of CPW-typed S.I. GaAs PCS as a function of bias voltage.

can provide additional insights on material properties, as these affect the radiation mechanism. One model describes optically excited THz radiation (OETR) as the dipole radiation of a time-dependent current of accelerated carriers in the static depletion field near the semiconductor surface (Hu *et al.*

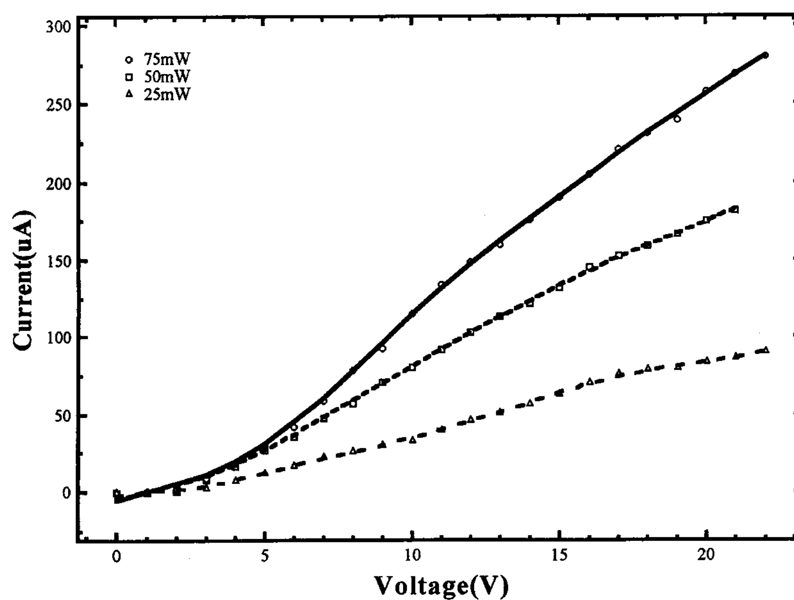

Fig. 10. The photocurrent of GaAs:H^+ PCS at different optical injection levels (25, 50 and 75 μW) is plotted as a function of biased voltage.

1991; Zhang and Auston 1992). According to this model, the radiated THz field, $E_{\rm rad}$ can be written as

$$E_{\rm rad}(t) \propto \frac{\partial}{\partial t}J(t) = e\eta n_{\rm ph}(t)\frac{\partial V_{\rm drift}(t)}{\partial t} + e\eta V_{\rm drift}(t)\frac{\partial n_{\rm ph}(t)}{\partial t} \approx e\eta V_{\rm drift}\frac{\partial n_{\rm ph}(t)}{\partial t} \propto \frac{e\eta V_{\rm drift} n_{\rm ph}(t)}{\tau_{\rm ph}} \quad (5)$$

where $E_{\rm rad}$ is the amplitude of transient THz field; $J(t)$ is the transient photocurrent, η is the product of optical quantum efficiency and other device related constants; $V_{\rm drift} \equiv \mu_{\rm eff} \cdot E_{\rm surface}$ denotes the drift velocity of photo-excited carriers, $\mu_{\rm eff}$ is the effective carrier mobility of the sample; $E_{\rm surface}$ is the surface depletion field near the semiconductor surface; $n_{\rm ph}(t) \approx n_0 e^{-t/\tau_c}$ is the transient photo-excited carrier density; and τ_c is the photo-excited carrier lifetime. The other model (Hu *et al.* 1991) states that the photo-excited electron–hole pairs are polarized by the dc electric field and give rise to a time-dependent polarization in the depletion layer. The time derivative of the polarization is the displacement current that can also emit THz radiation. In non-centro-symmetric crystals such as GaAs, second-order or third-order non-linear optical frequency mixing can also result in THz radiation by optical rectification of the excitation pulse (Greene *et al.* 1992):

$$P_i(t) = C_1 \sum_{jk} \chi^0_{ijk}(0; -\omega, \omega) E^\omega_j(t) E^\omega_k(t) + C_2 \sum_{jkl} \chi^0_{ijkl}(0; 0, -\omega, \omega) E^0_j E^\omega_k(t) E^\omega_l(t)$$

$$E_{\rm rad}(\theta, t) \sim \frac{\partial^2}{\partial t^2} P(\theta, t) \propto \sin^2\theta \cdot \frac{\partial^2 P_i(t)}{\partial t^2} \quad (6)$$

where $P_i(t)$ denotes the time-solved polarization change due to second- and/or third-order optical rectification effects; χ^0_{ijk} and χ^0_{ijkl} are the second and third order non-linear susceptibility coefficients, $\{E_j(t), E_k(t)\}$ and $\{E_k(t), E_l(t)\}$ denote the orthogonally polarized optical field, and E^0_j denotes the surface field of semiconductor. Clearly, we may always write the radiated field as the first time derivative of a current $J(t) = {\rm d}P(t)/{\rm d}t$ or the second time-derivative of a transient polarization $P(t)$.

Since high-order optical rectification effects can only occur on (1 1 0)- or (1 1 1)-oriented GaAs semiconductor substrate, OETR from (1 0 0)-oriented GaAs:H^+ substrate should be dominated by current surge effect. The radiated THz field can then be expressed in terms of the effective carrier mobility, $\mu_{\rm eff}$ and the time-dependent carrier density of the material, by using the Ohm's law. That is,

$$E_{\rm rad}(t) \propto \frac{\partial J(t)}{\partial t} \approx \frac{e\eta\mu_{\rm eff}(t)n_{\rm ph}(t)E_{\rm surface}}{\tau_{\rm c}} \cong \frac{I_{\rm photo}(t)}{1.2\times 10^{-6}\cdot P_{\rm in}(t)} \quad (7)$$

where $E_{\rm surface}$ denotes the strength of the surface depletion field, $\tau_{\rm c}$ denotes the lifetime of the photo-excited carriers, $I_{\rm photo}(t)$ is the electro-optic sampled transient photo-current measured by the lock-in amplifier in Fig. 11, and $P_{\rm in}(t)$ is the power of reflected optical probe beam incident into the photodetector. The effective carrier mobility of GaAs:H^+ can thus be calculated from the OETR data using Equation (7).

Figure 11 shows the OETR from GaAs:H^+ and S.I. GaAs substrates with the surface normal tilted at an angle $\theta_{\rm t} = 70°$ with respect to optical axis. Clearly, the peak amplitude of the emitted THz field became strongly attenuated hydrogen-ion-implantation process. The positive and negative peak values of the peak values of the electro-optic sampled photocurrent induced by the OETR from GaAs:H^+ are respectively 2.7 and −4 nA. The corresponding peak amplitudes of THz field were calculated to be 14 and −21 mV/cm by using equation (7). The relatively small THz field is due to the amorphous structure of the GaAs:H^+ material that leads to the reductions of carrier lifetimes and mobilities after implantation. The evidence for the amorphous structure of GaAs:H^+ has been reported elsewhere by using transmission electron microscopy (TEM) (Shober *et al.* 1992). In comparison, the THz radiation from an unbiased S.I. GaAs generates larger negative

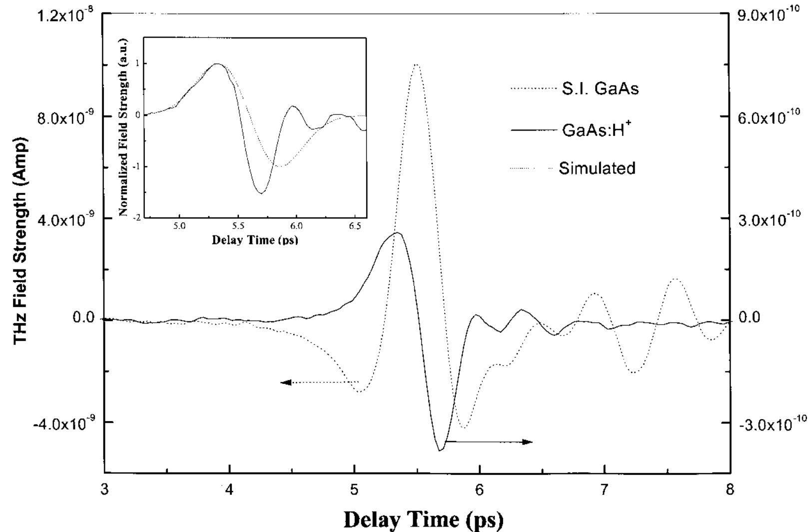

Fig. 11. The optically excited THz radiation from GaAs:H^+ (———) and S.I. GaAs (··············) substrates measured at $\theta_{\rm t} = 70°$. The (- - - -) in the inset figure illustrated the THz radiation simulated by a first-order derivative of the auto-correlated, Gaussian-shaped pulse of laser.

and positive peak currents of about −3.3 and 9.2 nA. These correspond to peak radiated field strengths of −190 and 520 mV/cm, respectively. Substituting these values in Equation (7), we deduce that the ratio of carrier mobilities for as-implanted GaAs:H^+ and S.I. GaAs is about 1:10^4. Since the carrier mobility of a commercial S.I. GaAs wafer is 8000 cm^2/V-sec (as specified by the manufacturer, American Xtal Technology, AXT), we estimate that the effective carrier mobility of our as-implanted GaAs:H^+ sample to be <1 cm^2/V-sec. This value is somewhat smaller but of the same order the as-implanted GaAs:H^+ material (about 5 cm^2/V-sec) (Lin and Pan 1999). The temporal response (FWHM) of the OETR waveform from GaAs:H^+ was only about 0.7 ps. In comparison, the temporal response of S.I. GaAs is larger than 1 ps with strongly oscillating tail response (see Fig. 11). With respect to that of S.I. GaAs, the phase of the radiated THz field pattern in GaAs:H^+ is reversed. Similar behavior was previously reported in other damaged material such as GaAs:N^+ (Shen *et al.* 1994) and GaAs:As^+ (Lin and Pan 1999). As in the case of GaAs:N^+, we interpret the phenomenon as consequence of reversal of the surface depletion field. That is, the implanted region changed from semi-insulating to n-type after the proton bombarding process.

In order to understand the THz radiating mechanism, magnetic field is applied (Zhang *et al.* 1993). Previously, the influence of magnetic fluid on the switching and improving the THz radiation from GaAs semiconductors has been reported by Zhang *et al.* (1993a, b). The results for GaAs:H^+ and S.I. GaAs are shown in Fig. 12. Also shown is a simulated curve, which is a first-

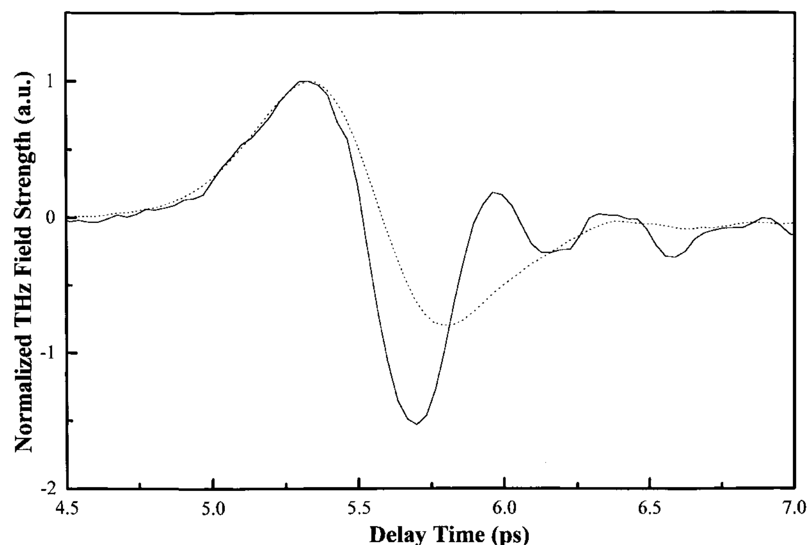

Fig. 12. The normalized THz radiation pulses from GaAs:H^+ (———) and S.I. GaAs (··············) measured at $\theta_t = 0°$.

order derivative of the auto-correlation trace of the laser pulse (a hyperbolic second function). The last one simulates an optically excited, ideal THz pulse that excludes the material response (i.e. carrier lifetime). It is found that the THz radiation from S.I. GaAs exhibits very similar shape with the ideal THz pulse except for a slightly different falling part. This is attributed to the longer decay time of photocurrent in S.I. GaAs ($\tau_c \approx 100$ ps) as compared to the FWHM of the auto-correlation function of the laser pulses ($\tau_c \approx 250$ fs). Furthermore, the nearly symmetric THz pulse shape indicates that the current surge effect is the dominant THz radiating mechanism for S.I. GaAs. In comparison, the optically-excited THz signal from GaAs:H^+ (see Fig. 12) is asymmetric and exhibits damping oscillation. The frequency of the damping oscillation is about 2.6 ± 0.1 GHz. We have tentatively attributed this spectral feature to shallow-level defects in GaAs:H^+ rather than the longitudinal optical phonons in either GaAs substrate or ZnTe sensor. The larger negative peak of THz field for GaAs:H^+ sample suggest that, due to the dense ion-implantation process, an additional radiating mechanism might be present other than the current surge effect. Another possibility is that the ultrafast carrier scattering process dramatically reduces the tail of photocurrent generated in GaAs:H^+. Note that the only difference in the THz radiation waveforms obtained at different θ_t, as shown in Figs. 11 and 12, is a slightly enhanced damping oscillation. The broadened power spectrum with 3 dB bandwidth of 1.29 THz for the OETR of GaAs:H^+ measured at normal incidence versus $\sim$1 THz for that measured at tilted angle of 70° can be explained by the magnetic field enhancement effect. (see Fig. 13) These

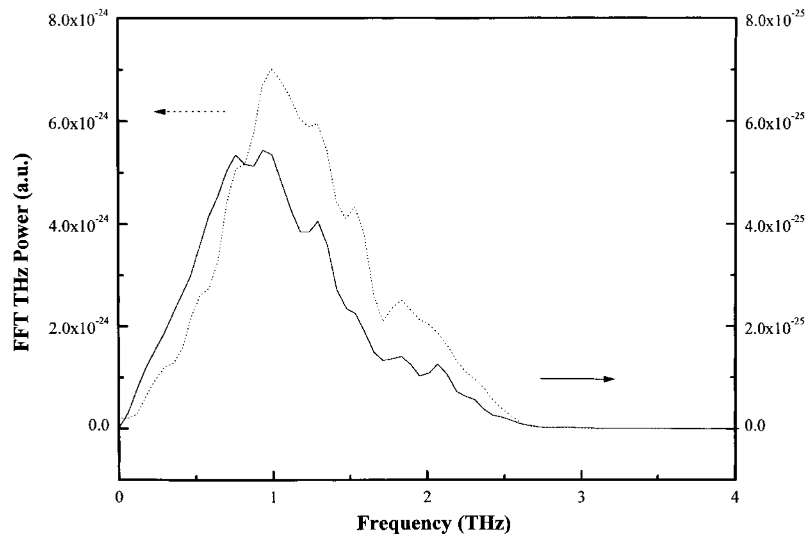

Fig. 13. The spectrum of the OETR from GaAs:H^+ (————) and S.I. GaAs (··················).

results again confirm the completely amorphous structure of the bombarded region. We therefore rule out the possibility of surface optical rectification effect as being another mechanism of THz radiation in GaAs:H^+.

6. Summary

We have investigated the ultrafast optical and optoelectronic characteristics of multi-energy proton-bombarded semi-insulating GaAs (GaAs:H^+) material and devices in some detail. The transient optical reflectivity of GaAs:H^+, as that of GaAs:As^+, was opposite in sign to that of S.I. GaAs. The maximum change on transient optical reflectivity and refractive index of GaAs:H^+ was determined to be -1×10^{-3} and -3×10^{-3} at wavelength of 865 nm. The latter is small as compared to the unprocessed S.I. GaAs ($> 1 \times 10^{-2}$), but slightly larger than but of the same of order of magnitude as LT-GaAs or GaAs:As^+ ($< 2 \times 10^{-3}$) material. Carrier lifetimes of GaAs implanted with protons at a single-dosage and multiple energies were observed to be as low as 350 $\pm$ 50 fs. The ultrashort carrier lifetime is attributed to the deep-level (EL2-like) defects that function as trapping centers in the as-implanted regions. Using the Shockley-Read-Hall model, we estimate that the density of trapping centers was about 3×10^{19} cm^{-3}. Ultrafast photoconductive switches (PCS) were successfully fabricated on GaAs:H^+. The temporal responses of CPW-typed and CPS-typed GaAs:H^+ PCSs were measured to be of 2.5 and 2 ps at FWHM, respectively. The corresponding 3 dB bandwidth of the CPS GaAs:H^+ PCS is greater than 150 GHz. This was presently limited by the temporal resolution of the electro-optical sampling system, estimated to be about 1.5 ps. The dark current of the GaAs:H^+ PCS was as low as 15 nA at a biased voltage, $V_{bias} \sim 10$ V, and was as low as 60 nA at biased voltage with $V_{bias} \sim 50$ V. Such low leakage current with a creeping current–voltage characteristics indicates that the as-implanted GaAs:H^+ may withstand much higher electric field before breakdown. Optically excited terahertz (THz) radiation from GaAs:H^+ was reported for the first time to our knowledge. The temporal response, center frequency and spectral bandwidth of the emitted THz radiation were 0.7 ps, 1 and 1.25 THz, respectively. The latter two figures are somewhat higher and larger than those reported for other defect-rich GaAs materials. From waveform analysis, we have tentatively attribute the primary physical mechanism responsible for the OETR from GaAs:H^+ as the current surge effect. The direction of depletion field near GaAs:H^+ surface was reversed due to high density of deep-level defects in the implanted region. The peak amplitudes of the positive and negative OETR fields estimated to be 14.7 and −22 mV/cm, respectively. The relatively small field amplitude is due to the amorphous surface layer. From the THz data, we are able to deduce that the effective

carrier mobility of GaAs:H^+ was less than 1 cm^2/V-sec. In conclusion, we demonstrated that multi-energy-implanted GaAs:H^+ is suitable for many of the applications in ultrafast optoelectronics. Further studies should improve its ultrafast characteristics.

Acknowledgement

This work was supported in part by the National Science Council of the Republic of China. The experimental data in Figs. 5 and 9 were taken by Mr S.-J. Yen. Technical Support by Prof. C.-S. Chang is also gratefully acknowledged.

References

Anonymous. Special Issue on Low Temperature Grown GaAs and Related Materials. *J. Electronic Mater.* **22**(12) Dec. 1993.

Anonymous. Special Issue on the Optical and Electron-Beam Control of Semiconductor Switches. *IEEE Trans. Electron Devices* **37**(12) 1990.

Chen, Y., S. Williamson, T. Brook, F.W. Smith and A.R. Calawa. 375-GHz-Bandwidth Photoconductive Detector. *Appl. Phys. Lett.* **59** 1984–1986, 1991.

Chou, S.Y., Y. Liu, W. Khalil, T.Y. Hsiang and S. Alexandrou. Ultrafast Nanoscale Metal-Semiconductor-Metal Photodetectors on Bulk on Low-Temperature Grown GaAs. *Appl. Phys. Lett.* **61**(7) 819–821, 1992.

Claverie, A., F. Namavar and Z. Liliental-Weber. Formation of As Precipitates in GaAs by Ion Implantation and Thermal Annealing. *Appl. Phys. Lett.* **62** 1271–1273, 1993a.

Claverie, A., F. Namavar, Z. Lilienthal-Weber, P. Dreszer and E.R. Weber. Semi Insulating GaAs Made by As Implantation and Thermal Annealing. *Mater. Sci. and Eng. B* **22** 37–40, 1993b.

Ejimanya, J.I. Current–Voltage Characteristics of Proton-Bombarded Au-GaAs Contacts. *Solid State Electron.* **29** 841–844, 1986.

Esser, A., W. Kutt, M. Strahnen, G. Maidorn and H. Kurz. Femtosecond Transient Reflectivity Measurements as a Probe for Process-Induced Defects in Silicon. *Appl. Surf. Sci.* **46** 446–450, 1990.

Ganikhanov, F., G.-R. Lin, W.-C. Chen, C.-S. Chang and C.-L Pan. Subpicosecond Carrier Lifetime in Arsenic-Ion-Implanted GaAs. *Appl. Phys. Lett.* **67** 3465–3467, 1995.

Greene, B.I., P.N. Saeta, D.R. Dykaar, S. Schmitt-Rink and S.L. Chuang. Far-Infrared Light Generation at Semiconductor Surfaces and Its Spectroscopic Applications. *IEEE J. Quantum Electron.* **28** 2302–2312, 1992.

Hu, B.B., X.-C. Zhang and D.H. Auston. Terahertz Radiation Induced by Subband-Gap Femtosecond Optical Excitation of GaAs. *Phys. Rev. Lett.* **67** 2709–2712, 1991.

Johnson, M.B., T.C. McGill and N.G. Paulter. Carrier Lifetimes in Ion-damaged GaAs. *Appl. Phys. Lett.* **54** 2424–2426, 1989.

Kaminska, M., E.R. Weber, Z. Lilental-Weber, R. Leon and Z.U. Rek. Stoichiometry-Related Defects in GaAs Grown by Molecular-Beam Epitaxy at Low Temperatures. *J. Vac. Sci. Technol. B* **4** 710–713, 1989.

Krotkus, A., S. Marcinkevicius, J. Jasinski, M. Kaminska, H.H. Tan and C. Jagadish. Picosecond Carrier Lifetime in GaAs Implanted with High Doses of As ions: an Alternative Material to Low-Temperature GaAs for Optoelectronic Applications. *Appl. Phys. Lett.* **66** 3304–3306, 1995.

Krotkus, A., S. Marcinkevicius, J. Jasinski, M. Kaminska, H.H. Tan and C. Jagadish. Picosecond Carrier Lifetime in GaAs Implanted with High Doses of As ions: an Alternative Material to Low-Temperature GaAs for Optoelectronic Applications. *Appl. Phys. Lett.* **66** 3304–3306, 1995.

Lambsdroff, M., J. Kuhl, J. Rosenzweig, A. Axmann and J. Schneider. Subpicosecond Carrier Lifetimes in Radiation-Damaged GaAs. *Appl. Phys. Lett.* **58** 1881–1883, 1991.

Lin, G.-R. and C.-L. Pan. Picosecond Responses of Low-dosage Arsenic-Ion-Implanted GaAs Photoconductors. *Appl. Phys. Lett.* **71** 2901–2903, 1997.

Lin, G.-R. and C.-L. Pan. Characterization of Optically Excited THz Radiation from Arsenic-ion-implanted GaAs. *Appl. Phys. B*, 1999.

Lin, G.-R., W.-C. Chen, C.-S. Chang and C.-L. Pan. Electrical Characterization of Arsenic-Ion-Implanted Semi-Insulating GaAs by Current–Voltage Measurement. *Appl. Phys. Lett.* **65** 3272–3274, 1994.

Lin, G.-R., W.-C. Chen, S.-C. Chou, C.-S. Chang, K.-H. Wu and C.-L. Pan. Material and Ultrafast Optical Characterization of High-Resistive Arsenic-Ion-Implanted GaAs. *IEEE J. Quantum Electron.* **34** 1740–1748, 1998.

Lochtefeld, A.J., M.R. Melloch, J.C.P. Chang and E.S. Harmon. The Role of Point Defects and Arsenic Precipitates in Carrier Trapping and Recombination in Low-Temperature Grown GaAs. *Appl. Phys. Lett.* **69** 1465–1467, 1996.

Look, D.C., D.C. Walters, M.O. Manasreh, J.R. Sizelove and C.E. Stutz. Anomalous Hall-Effect Results in Low-Temperature Molecular-Beam-Epitaxy GaAs: Hopping in a Dense EL-2 Like Band. *Phys. Rev. B* **42** 3578–3581, 1990.

McIntosh, K.A., K.B. Nichols, S. Verghese and E.R. Brown. Investigation of Ultrashort Photocarrier Relaxation Times in Low-Temperature-Grown GaAs. *Appl. Phys. Lett.* **70** 354–356, 1997.

Paulter, N.G., A.J. Gibbs and D.N. Sinha. Fabrication of High-Speed GaAs Photoconductive Pulse Generators and Sampling Gates by Ion Implantation. *IEEE Trans. Electron. Dev.* **65** 2343–2348, 1988.

Schumacher, H., U. Salz and H. Beneking. Fast GaAs Photoconductive Detectors with High Sensitivity Integrated in Coplanar Systems onto GaAs Substrate. In *Picosecond Electronics and Optoelectronics II*, eds. Leonberger, F.J., C.H. Lee, F. Capasso and H. Morkoc, 209–213, 1987.

Shen, H., Y. Jin, G.A. Wagoner, X.-C. Zhang and L. Kingsley. Time-resolved Optoelectronic Measurements of Nitrogen-Implanted GaAs. Ultrafast Phenomena IX, Springer Series in Chemical Physics, vol. 60, pp. 372–374, Springer-Verlag Berlin Heidelberg, 1994.

Shober, T., J. Friedrich and A. Altmann. Proton Implantation into GaAs: Transmission Electron Microscopy Results. *J. Appl. Phys.* **71** 2206–2210, 1992.

Smith, R.A. Semiconductors. 2nd edn, Chap. 9 273–279, Cambridge University Press, 1978.

Smith, F.W., H.Q. Le, V. Diaduik, M.A. Hollis, A.R. Calawa, S. Gupta, M. Frankel, D.R. Dykaar, G.A. Mourou and T.Y. Hsiang. Picosecond GaAs Based Photoconductive Optoelectronic Detectors. *Appl. Phys. Lett.* **54** 890–892, 1989.

Tan, H.H., J.S. Williams and C. Jagadish. Characterization of Deep Levels and Carrier Compensation Created by Proton Irradiation in Undoped GaAs. *J. Appl. Phys.* **78** 1481–1487, 1995.

Verghese, S., N. Zamdmer, Q. Hu, E.R. Brown and A. Forster. An Optical Correlator Using a Low-Temperature-Grown GaAs Photoconductor. *Appl. Phys. Lett.* **69** 842–844, 1996.

Wang, H.-H., P. Grenier, J.F. Whitaker, H. Fujioka, J. Jasinski and Z. Liliental-Weber. Ultrafast Response of As-Implanted GaAs Photoconductors. *IEEE J. Sel. Top. Quantum Electron.* **2** 630–635, 1996.

Warren, A.C., J.M. Woodall, D.T. McInturff, R.T. Hodgson and M.R. Melloch. 1.3-μm P-i-N Photodetector Using GaAs with Precipitates (GaAs:As). *IEEE Electron. Device. Lett.* **12** 527–529, 1991.

Wu, Q., and X.-C. Zhang. Free Space Electro-Optic Sampling of Terahertz Beams. *Appl. Phys. Lett.* **68** 1604–1606, 1996.

Zhang X.-C. and D.H. Auston. Optoelectronic Measurement of Semiconductor Surfaces and Interfaces with Femtosecond Optics. *J.Appl. Phys.* **71** 326–338, 1992.

Zhang, X.-C., B.-B. Hu, J.T. Darrow and D.H. Auston. Generation of Femtosecond Electromagnetic Pulses from Semiconductor Surfaces. *Appl. Phys. Lett.* **56** 1011–1014, 1990.

Zhang, X.-C., Y. Jin, T.D. Hewitt and T.Sangsiri. Magnetic Switching of THz beam. *Appl. Phys. Lett.* **62** 2003–2005, 1993a.

Zhang, X.-C., Y. Jin, L.E. Kinsley and M. Weiner. Influence of Electric and Magnetic Field on THz radiation. *Appl. Phys. Lett.* **62** 2477–2479, 1993b.